

# Upper critical dimension for irreversible cluster nucleation and growth in the point-island regime

 Feng Shi,<sup>\*</sup> Yunsic Shim,<sup>†</sup> and Jacques G. Amar<sup>‡</sup>
*Department of Physics & Astronomy, University of Toledo, Toledo, Ohio 43606, USA*

(Received 28 December 2005; revised manuscript received 19 June 2006; published 29 August 2006)

We compare the results of kinetic Monte Carlo (KMC) simulations of a point-island model of irreversible nucleation and growth in four dimensions (4D) with the corresponding mean-field (MF) rate-equation predictions for the monomer density, island density, island-size distribution (ISD), capture-number distribution (CND), and capture-zone distribution (CZD), in order to determine the critical dimension  $d_c$  for mean-field behavior. The asymptotic behavior is studied as a function of the fraction of occupied sites (coverage) and the ratio  $D/F$  of the monomer hopping rate  $D$  to the (per site) monomer creation rate  $F$ . Excellent agreement is found between our KMC simulation results and the MF rate equation results for the average island and monomer densities. For large  $D/F$ , the scaled CND and CZD do not depend on island size, in good agreement with the MF prediction, while the scaled ISD also agrees well with the MF prediction except for a slight difference at the peak values. Coupled with previous results obtained in  $d=3$ , these results indicate that for growth in the point-island regime, the upper critical dimension for irreversible cluster nucleation and growth is equal to 4.

 DOI: [10.1103/PhysRevE.74.021606](https://doi.org/10.1103/PhysRevE.74.021606)

PACS number(s): 81.15.Aa, 68.55.Ac, 68.43.Jk

## I. INTRODUCTION

Due to its broad technological importance a great deal of experimental [1–10] and theoretical [11–30] effort has been carried out toward obtaining a better understanding of cluster nucleation in submonolayer epitaxial growth. In particular, the scaling properties of the island-size distribution  $N_s(\theta)$  (where  $N_s$  is the number of islands of size  $s$  at coverage  $\theta$ ) have drawn much attention [11–30]. In the precoalescence regime the island-size distribution satisfies the scaling form [14,15]

$$N_s(\theta) = \frac{\theta}{S^2} f\left(\frac{s}{S}\right), \quad (1)$$

where  $S$  is the average island size, and the scaling function  $f(u)$  depends on the critical island size and island morphology [18].

A standard approach to nucleation and growth is provided by the use of rate equations (REs) [11,12,31]. Such an approach has also been applied to a variety of other diffusion-mediated processes including coagulation and chemical reactions [32]. For the case of irreversible growth, rate equations valid in the precoalescence regime may be written in the form

$$\frac{dN_1}{d\theta} = 1 - 2R\sigma_1 N_1^2 - RN_1 \sum_{s=2}^{\infty} \sigma_s N_s - \kappa_1 N_1 - \sum_{s=1}^{\infty} \kappa_s N_s, \quad (2)$$

$$\frac{dN_s}{d\theta} = R\sigma_{s-1} N_1 N_{s-1} - R\sigma_s N_1 N_s + \kappa_{s-1} N_{s-1} - \kappa_s N_s \quad (s \geq 2), \quad (3)$$

where  $R=D/F$  is the ratio of the monomer diffusion rate  $D$  to the (per site) deposition rate  $F$ , the terms with  $\kappa_s$  correspond to direct impingement, and the capture numbers  $\sigma_s$  ( $\sigma_1$ ) correspond to the *average* capture rate of diffusing monomers by islands of size  $s$  (monomers). Using this approach and assuming scaling, Bartelt and Evans have shown [19] that in the asymptotic limit of infinite  $D/F$ , the scaled island-size distribution (ISD) is related to the scaled capture-number distribution (CND) as

$$f(u) = f(0) \exp\left(\int_0^u dx \frac{2z-1-C'(x)}{C(x)-zx}\right), \quad (4)$$

where  $C(s/S) = \sigma_s / \sigma_{av}$  is the scaled CND,  $z$  is the dynamical exponent describing the dependence of the average island size on coverage ( $S \sim \theta^z$ ), and  $f(0)$  is determined by the normalization condition  $\int_0^\infty du f(u) = 1$ . We note that for the case of irreversible growth of point islands as is considered here, one has  $z=2/3$ .

The simplest possible assumption for the CND is the mean-field (MF) assumption that the capture number is independent of island size, i.e.,  $\sigma_s = \sigma_{av}(\theta)$  or  $C(u) = 1$ . Using Eq. (4), for the case of irreversible growth ( $z=2/3$ ) this leads to the MF prediction for the asymptotic scaled ISD  $f_{MF}(u) = (1/3)(1-2u/3)^{-1/2}$  for  $0 < u < 3/2$  which diverges at  $u_c^{MF} = 3/2$ . However, for the case of irreversible submonolayer growth on a two-dimensional (2D) substrate ( $d=2$ ) it has been shown [19] that, even for point islands, due to correlations between the island size and the size of its surrounding capture zone, the MF assumption does not hold, i.e., the asymptotic CND depends strongly on island size. As a result, the asymptotic scaled ISD does not diverge in  $d=2$ . Since with increasing dimension  $d$  one expects that the effects of

<sup>\*</sup>Electronic address: fengshi@physics.utoledo.edu

<sup>†</sup>Electronic address: yshim@physics.utoledo.edu

<sup>‡</sup>Electronic address: jamar@physics.utoledo.edu

such correlations will decrease, the question then arises, what happens for  $d > 2$ , and in particular what is the critical dimension  $d_c$  for MF behavior in irreversible nucleation and growth?

In order to address these questions, we have recently carried out kinetic Monte Carlo (KMC) simulations of a point-island model of irreversible growth in three dimensions (3D) ( $d=3$ ) [33]. We note that this model may also be thought of as a simplified model of vacancy formation and vacancy cluster nucleation during irradiation. Surprisingly, we found that while the scaled capture number distribution  $C(u)$  is close to the MF prediction (and as a result the asymptotic ISD diverges with increasing  $D/F$ ) for large  $D/F$  both the scaled ISD and CND differ from the MF predictions. In particular, due to geometric effects in 3D, the scaled ISD diverges more slowly than the MF prediction while the asymptotic divergence occurs at a value of the scaled island size, which is somewhat larger than the MF prediction. These results suggest that the critical dimension  $d_c$  for MF behavior is larger than 3.

Here we present the results of KMC simulations of a point-island model of irreversible growth carried out in  $d=4$  in order to compare with MF predictions. For comparison, the results of a self-consistent MF RE calculation are also presented and compared with the corresponding simulation results for the average island density  $N$ , monomer density  $N_1$ , island-size distribution, and capture-number distribution. Our results indicate that, due to the decreased role of correlations in 4D, the asymptotic scaled CND, capture-zone distribution (CZD), and ISD are in good agreement with the MF prediction in  $d=4$ . These results indicate that the upper critical dimension for irreversible nucleation and growth is  $d_c=4$ .

This paper is organized as follows. In Sec. II we first describe our simulations. In Sec. III we present our self-consistent MF rate-equation approach. In Sec. IV, we present a comparison between our self-consistent MF RE calculations and KMC results for the average island and monomer densities. We then present our KMC results for the scaled ISD, CND, and CZD along with a comparison with MF theory. Finally, we discuss and summarize our results in Sec. V.

## II. MODEL AND SIMULATIONS

In order to study the scaling behavior of the ISD, CND, and CZD in 4D, we have used a simple point-island model of irreversible nucleation and growth. Our model is a straightforward analog of the corresponding point-island model previously studied in two dimensions [19]. In our model, monomers are created at random sites on a 4D cubic lattice with rate  $F$  per site per unit time, and then hop randomly in each of the eight nearest-neighbor directions with hopping rate  $D_h$ . If a monomer lands on a site already occupied by another monomer or is created at such a site, then a dimer island is nucleated. Similarly, if a monomer lands on or is created at a site already occupied by an island then that monomer is captured by that island and the island size increases by 1. The key parameter in this model is the ratio  $R_h = D_h/F$  of the

monomer hopping rate to the (per site) monomer creation rate, or equivalently the ratio  $R = D/F = R_h/8$ .

In order to study the asymptotic scaling behavior, we have carried out simulations over a range of values of  $R_h$  ranging from  $10^5$  to  $10^{10}$  and with system sizes ranging from  $L=40$  to 100. Our results were typically averaged over 200 runs to obtain good statistics. For each set of parameters the scaled ISD, CND, and CZD were obtained for coverages ranging from  $\theta=0.1$  to 0.4, while the average island density  $N(\theta)$  and monomer density  $N_1(\theta)$  were also measured. We note that in order to measure the capture-number distribution, the method outlined in Ref. [19] was used. In particular, the capture number  $\sigma_s(\theta)$  was calculated using the expression  $\sigma_s(\theta) = n_s^c / (R \Delta \theta N_1 N_s L^4)$  where  $n_s^c$  is the number of monomer capture events corresponding to an island of size  $s$  during a very small coverage interval ( $\Delta \theta \approx 0.001$ ). As in Ref. [19] the island size  $s$  at the beginning of the coverage interval was used when incrementing the counter  $n_s^c$  in order to obtain good statistics. We also note that in our capture-zone distribution calculations, the capture zone  $v$  of an island was defined as corresponding to all monomer sites or empty sites which are closer to that island than any other island. If such a site was equally close to several islands, then that site's contribution to the capture zone was equally distributed between the islands.

## III. SELF-CONSISTENT RATE-EQUATION APPROACH

For the point-island model the island radius  $R_s$  is independent of island size  $s$ , i.e.,  $R_s = R_0$ . Accordingly, within the MF RE approach the capture numbers are assumed to be independent of island size  $s$  and may be written as  $\sigma_s = \sigma(\theta)$ . The coupled rate equations for the average monomer density  $N_1$  and island density  $N$  (where  $N = \sum_{s=2}^{\infty} N_s$ ) may then be written

$$\frac{dN_1}{d\theta} = 1 - 2N_1 - N - 2(D/F)\sigma N_1^2 - (D/F)\sigma N_1 N, \quad (5)$$

$$\frac{dN}{d\theta} = N_1 + 2(D/F)\sigma N_1^2. \quad (6)$$

In order to solve Eqs. (5) and (6), one has to obtain an expression for the capture numbers  $\sigma(\theta)$ . As in Ref. [17] in which a self-consistent RE approach to 2D irreversible nucleation and growth is discussed, we consider a quasistatic diffusion equation for the monomer density  $n_1(r, \theta, \phi)$  surrounding an island of size  $s$  of the form

$$\nabla^2 n_1(r, \theta, \phi) - \xi^{-2}(n_1 - N_1) = 0, \quad (7)$$

where  $N_1$  is the average monomer density and

$$\xi^{-2} = \sigma(N + 2N_1). \quad (8)$$

Assuming spherical symmetry Eq. (7) may be written in 4D,

$$\frac{1}{r^3} \frac{d}{dr} \left( r^3 \frac{d\tilde{n}_1}{dr} \right) - \xi^{-2} \tilde{n}_1(r) = 0 \quad (9)$$

where  $\tilde{n}_1(r) = n_1(r) - N_1$ . The general solution is given by

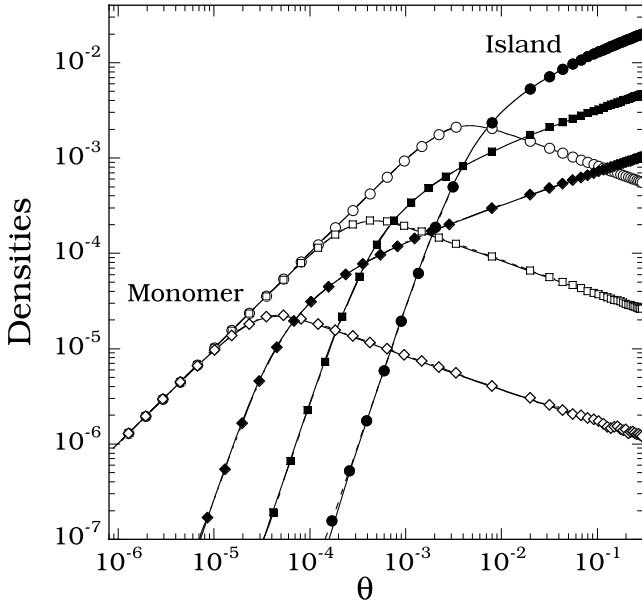


FIG. 1. Comparison between KMC results (symbols) and the corresponding self-consistent MF RE results (solid lines) for the monomer density  $N_1$  and island density  $N$  as a function of coverage for  $D_h/F=10^5$  (circles),  $10^7$  (squares), and  $10^9$  (diamonds).

$$\tilde{n}_1(r) = \left(\frac{\xi}{r}\right) \frac{d}{d(r/\xi)} [b_1 I_0(r/\xi) + b_2 K_0(r/\xi)], \quad (10)$$

where  $b_1$  and  $b_2$  are constants. Since  $\tilde{n}_1(r) \rightarrow 0$  as  $r \rightarrow \infty$ , one has  $b_1=0$  which implies that  $\tilde{n}_1(r) \sim \left(\frac{1}{r}\right) \xi K_1(r/\xi)$ . The irreversible growth boundary condition  $n_1(R_s)=0$  then leads to

$$n_1(r) = N_1 \left(1 - \frac{R_s}{r} \frac{K_1(r/\xi)}{K_1(R_s/\xi)}\right). \quad (11)$$

Equating the microscopic flux of atoms near the island  $S_v D[\partial n_1 / \partial r]_{r=R_s}$  (where  $S_v = 2\pi^2 R_s^3$  is the surface area of a sphere of radius  $R_s$  in 4D) to the corresponding macroscopic RE-like term  $DN_1 \sigma_s$ , we obtain an equation for the capture number,

$$\sigma_s = \frac{S_v}{N_1} \left(\frac{\partial n_1}{\partial r}\right)_{r=R_s} = 4\pi^2 R_s^2 \left(1 + \frac{R_s K_0(R_s/\xi)}{2\xi K_1(R_s/\xi)}\right). \quad (12)$$

Since for the point-island model considered here  $R_s=R_0$ , the corresponding capture numbers may be written

$$\sigma_s = \sigma = 4\pi^2 R_0^2 \left(1 + \frac{R_0 K_0(R_0/\xi)}{2\xi K_1(R_0/\xi)}\right) \quad (13)$$

where  $R_0$  is a model-dependent constant of order 1 and  $\xi$  is defined in Eq. (8). In the limit of infinite  $D/F$  one has  $R_0/\xi=0$ , which implies  $\sigma=4\pi^2 R_0^2$ , i.e., the capture numbers have no coverage dependence.

#### IV. RESULTS

Figure 1 shows a comparison between our KMC simulation results for the average monomer and island densities and the corresponding self-consistent MF RE results obtained by

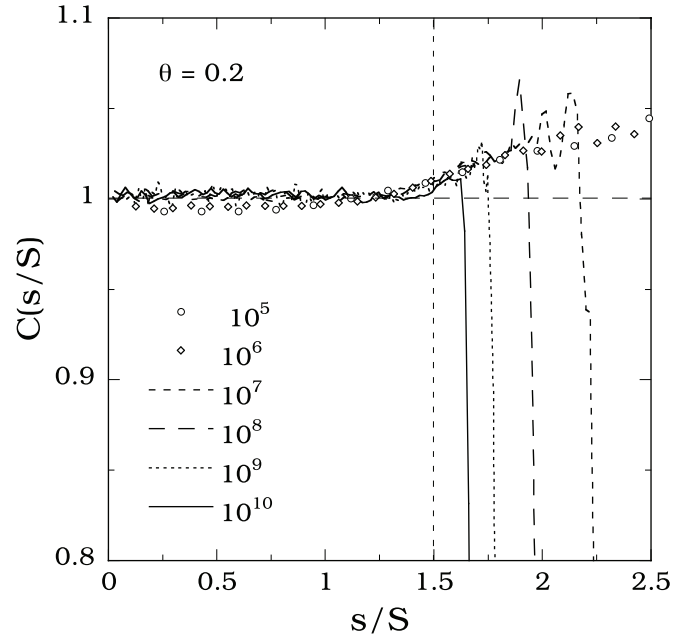


FIG. 2. KMC simulation results for scaled CND for  $D_h/F = 10^5 - 10^{10}$ . Horizontal dashed line corresponds to MF prediction.

numerically solving Eqs. (5) and (6) along with Eqs. (8) and (13). Results are shown for  $D_h/F=10^5, 10^7$ , and  $10^9$ , while the value of  $R_0$  ( $R_0=0.407$ ) was chosen to give the best fit to the KMC data. As can be seen, there is excellent agreement between the RE and KMC results over all coverages and for all values of  $D_h/F$ . Thus, as was previously found in  $d=2$  [17] and 3 [33], the self-consistent RE approach provides an accurate description for average quantities such as the monomer and island density. We note that these results also imply that the standard MF expressions for the dependence of the island density and monomer density on coverage and  $D/F$  apply, i.e.,  $N_1 \approx \theta, N \sim (D/F)\theta^3$  for  $\theta \ll \theta_x$  and  $N_1 \sim (D/F)^{-2/3} \theta^{-1/3}, N \sim (D/F)^{-1/3} \theta^{1/3}$  for  $\theta \gg \theta_x$ , where  $\theta_x \sim (D/F)^{-1/2}$  is the crossover coverage at which the island density exceeds the monomer density. We now compare our simulation results for the CND, ISD, and CZD with the corresponding MF rate-equation results.

Figure 2 shows the scaled capture number distribution  $C(s/S)$  obtained in our KMC simulations at coverage  $\theta = 0.2$  for  $D_h/F=10^5 - 10^{10}$ . The MF prediction  $C(u)=1$  is also shown (horizontal dashed line). As can be seen, in contrast to the significant deviations between the KMC results and the MF prediction observed in  $d=1$  [23],  $d=2$  [19], and  $d=3$  [33], the KMC results in 4D approach the MF prediction with increasing  $D_h/F$ . In particular,  $C(u)$  for  $D_h/F=10^{10}$  is approximately equal to 1 for  $u < 1.5$  while it increases slightly with  $u$  for  $u > 1.5$ . As already noted [see Eq. (4)], the MF prediction implies the existence of an asymptotic divergence in the scaled ISD at the point  $u_c^{MF}=3/2$  where the MF CND crosses the line  $2u/3$ . In order to find the corresponding asymptotic crossing point in our simulations, we have examined the point  $u_c^{KMC}(D/F)$  at which the scaled CND crosses the MF prediction  $C(u)=1$  for  $u > 3/2$  as a function of  $D/F$ . We find that the crossing point is well fitted by the form  $u_c^{KMC}(D/F) = u_c^{KMC}(\infty) + c(D/F)^{-\gamma}$  with  $u_c^{KMC}(\infty) \approx 1.50$

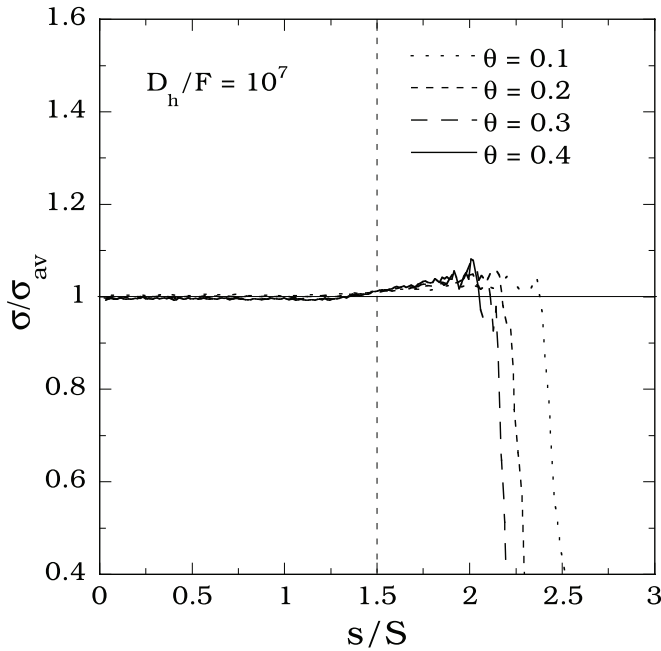


FIG. 3. KMC simulation results for scaled CND as a function of coverage for  $D_h/F=10^7$ . Horizontal dashed line corresponds to MF prediction.

and  $\gamma=0.22$ . This result indicates that the scaled CND exhibits pure MF behavior [i.e.,  $C(u)=1$  for  $0 < u < 3/2$ ] in the asymptotic limit of infinite  $D/F$ .

As shown in Fig. 3, we have also studied the dependence of the scaled CND on coverage  $\theta$  at fixed  $D_h/F=10^7$ . As can be seen, for fixed  $D/F$  the CND distribution also appears to gradually approach the MF prediction with increasing coverage. We note, however, that the asymptotic limit of very large coverage corresponds to an “unphysical” limit of large island density and small distance between islands and so is of less interest than the limit of large  $D/F$ .

We now consider the behavior of the scaled ISD as a function of  $D/F$ . Figure 4 shows a comparison between our KMC results (symbols) and the corresponding self-consistent MF RE results (solid curves) for the scaled ISD as a function of  $D/F$  at coverage  $\theta=0.2$ . The asymptotic MF result  $f(u) = \frac{1}{3}(1-2u/3)^{-1/2}$  [13,18] corresponding to infinite  $D/F$  is also shown (dashed curve). As expected, the scaled ISD becomes sharper and the peak of the scaled ISD increases with increasing  $D/F$ , thus indicating a divergence in the asymptotic limit of infinite  $D/F$ . In contrast to the 3D case [33], for the 4D case considered here, the KMC results are in very good agreement with the corresponding self-consistent MF RE results and approach the asymptotic MF prediction with increasing  $D/F$ . However, for large  $D/F$  there is a small difference of about 3.3% between the KMC peak values and the corresponding MF RE predictions. This difference may be explained by the fact that, while the scaled CND approaches the MF prediction in the limit of infinite  $D/F$ , for finite  $D/F$  there are still small deviations from the MF prediction. While such deviations become smaller for large  $D/F$  they are also more strongly amplified for large  $D/F$ . As a result, the relative differences between the MF RE

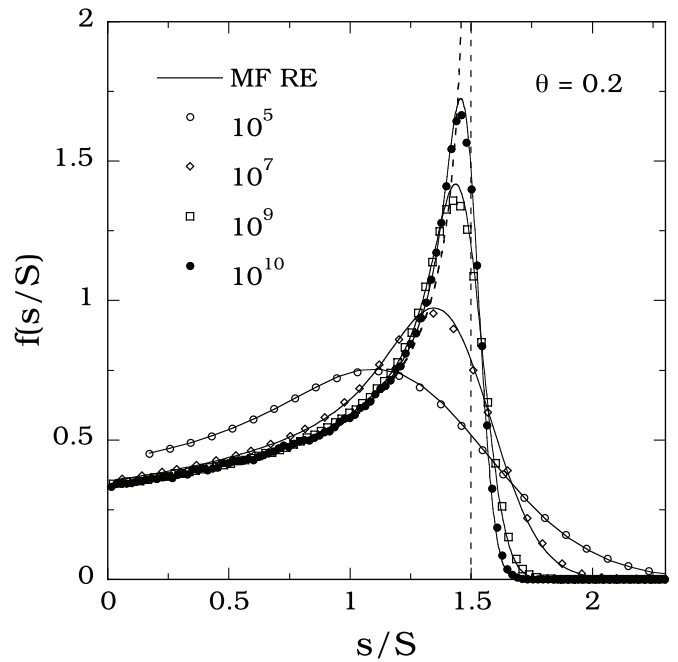


FIG. 4. Scaled ISDs for  $D_h/F=10^5, 10^7, 10^9,$  and  $10^{10}$ . KMC simulation results (symbols), RE results (solid lines), and asymptotic MF limit (dashed curve).

prediction and the KMC results are essentially independent of  $D/F$  for large  $D/F$ . Similar results have been obtained at lower coverage ( $\theta=0.1$ ) as well as at higher coverage ( $\theta=0.4$ ).

In order to understand this difference, in Fig. 5 we plot the peak values of the scaled ISD obtained from both KMC simulations and MF RE calculations as a function of  $D/F$  for two different coverages ( $\theta=0.2$  and  $0.4$ ). As can be seen, in

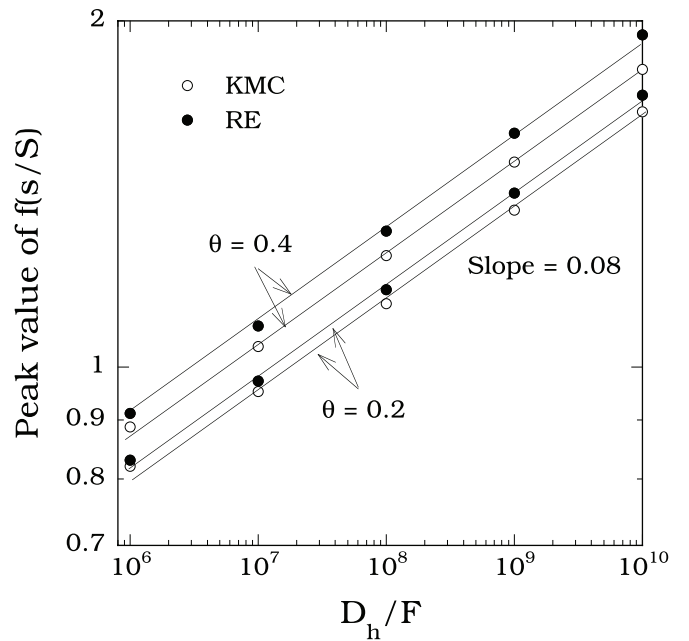


FIG. 5. Log-log plot of peak value of scaled ISD as function of  $D_h/F$  at different coverages.

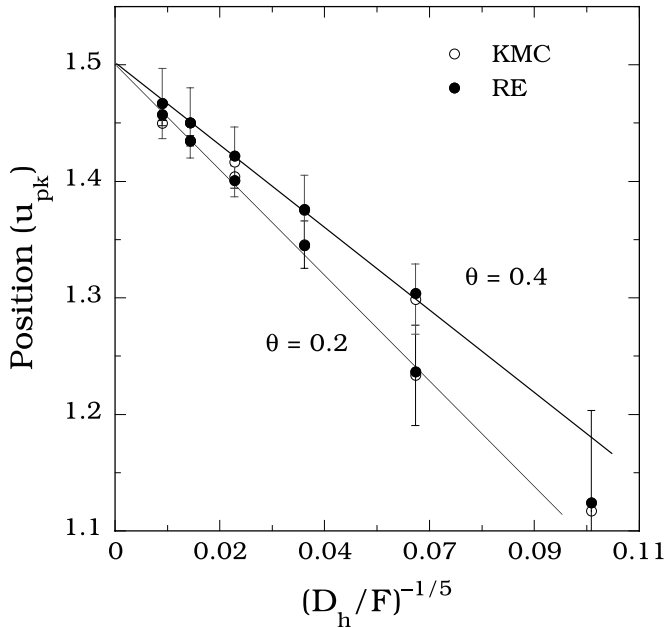


FIG. 6. Plot of  $u_{pk}(D/F)$  as a function of  $(D_h/F)^{-\gamma}$  for  $D_h/F$  ranging from  $10^5$  to  $10^{10}$ . Solid line is a fit as described in text with  $\gamma=1/5$ , and error bars are given for the KMC results.

both cases the peak value  $f_{pk}(D/F)$  of the scaled ISD increases as a power law with  $f_{pk} \sim (D/F)^\phi$ , thus indicating a divergent ISD in the asymptotic limit. However, in contrast to our previous results in  $d=3$  [33], the value of  $\phi$  obtained from the KMC simulations ( $\phi=0.081 \pm 0.005$ ) for  $D_h/F \geq 10^7$  is in excellent agreement with that obtained from our MF RE calculations ( $\phi=0.083 \pm 0.005$ ). Thus, in the asymptotic limit the scaled ISD obtained from KMC simulations is essentially the same as the MF prediction.

The asymptotic position  $u_{pk}$  of the ISD peak is also examined in Fig. 6 for two different coverages ( $\theta=0.2$  and  $0.4$ ). In order to extrapolate the asymptotic behavior, the peak position was fitted to the form  $u_{pk}(D/F) = u_{pk}^{(\infty)} + c(D/F)^{-\gamma}$  while the value of  $\gamma=1/5$  was used for the best fit. The results obtained from KMC simulations (open circles) as well from the MF RE predictions (filled circles) are shown. As can be seen, there is excellent agreement between the KMC and MF RE results at both coverages. In particular, for the MF RE and KMC results we find  $u_{pk}^{MF(\infty)} = 1.502$  and  $u_{pk}^{KMC(\infty)} = 1.50 \pm 0.02$ , respectively. Thus, in contrast to the corresponding KMC simulation results in 3D [33], the asymptotic peak position in 4D is in excellent agreement with the MF RE result.

We note that for finite  $D/F$  the peak of the ISD increases with increasing coverage as indicated in Fig. 5, and also shifts to the right (see Fig. 6). This is in agreement with the MF RE prediction [19] that the scaled ISD depends on both  $D/F$  and coverage. Accordingly, for the point-island model in 4D there is no true scaling of the ISD with coverage and  $D/F$  except in the limit of infinite  $D/F$  for which the resulting ISD diverges.

In order to further understand the observed MF behavior, we have also measured the scaled CZD  $v_s/v_{av} = B(s/S)$  for  $D_h/F = 10^5 - 10^9$ , where  $v_s$  is the size of the capture zone

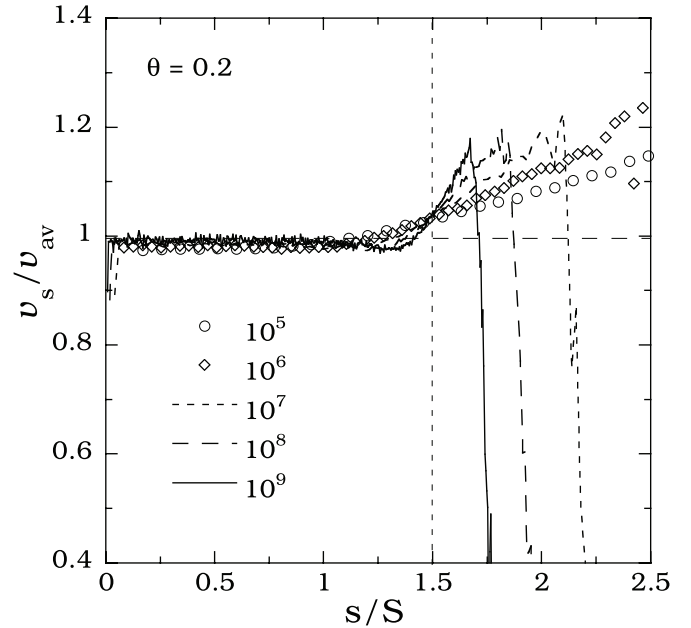


FIG. 7. KMC simulation results for scaled CZD for  $D_h/F = 10^5 - 10^9$ . Horizontal dashed line corresponds to MF CZD.

corresponding to an island of size  $s$ , and  $v_{av}$  is the size of the average capture zone. Figure 7 shows typical results obtained at coverage  $\theta=0.2$  with  $D_h/F$  ranging from  $10^5$  to  $10^9$ . The MF prediction  $B(u)=1$  is also shown (horizontal dashed line). As can be seen, the shape of the scaled CZD is similar to that of the scaled CND. In particular,  $B(u) \approx 1$  for  $u < 3/2$  while near  $u=3/2$  it increases rapidly with island size for large  $D/F$ . In addition, for large  $D/F$  the scaled CZD curves obtained from the KMC simulation appear to “pivot” with increasing  $D/F$  around a fixed point at  $u_c \approx 1.5$  which is also the point at which they cross. Similar results have been obtained at other coverages. In order to further understand the asymptotic behavior, and also exhibit the coverage dependence, in Fig. 8 we show the slope of each of the curves at the crossing point  $u=3/2$  as a function of  $D/F$  for coverages ranging from  $\theta=0.1$  to  $0.4$ . As shown in Fig. 8, the corresponding slope increases as a power law, i.e.,  $m_c(D/F) \sim (D/F)^{\phi'}$ , while the value of the exponent ( $\phi' \approx 0.2$ ) is essentially independent of coverage. This indicates that in the asymptotic limit of infinite  $D/F$ , the scaled CZD approaches the MF prediction.

## V. DISCUSSION

In our previous study of irreversible nucleation and growth in 3D [33], we found that due to the existence of (weak) correlations, the asymptotic scaled CND depends weakly on the island size and accordingly the asymptotic scaled ISD also differs somewhat from the MF prediction. In particular, we found that the scaled ISD diverges more slowly than the MF prediction while the asymptotic divergence occurs at a value of the scaled island size which is somewhat larger than the MF prediction. Based on these results we concluded that the critical dimension for MF behav-

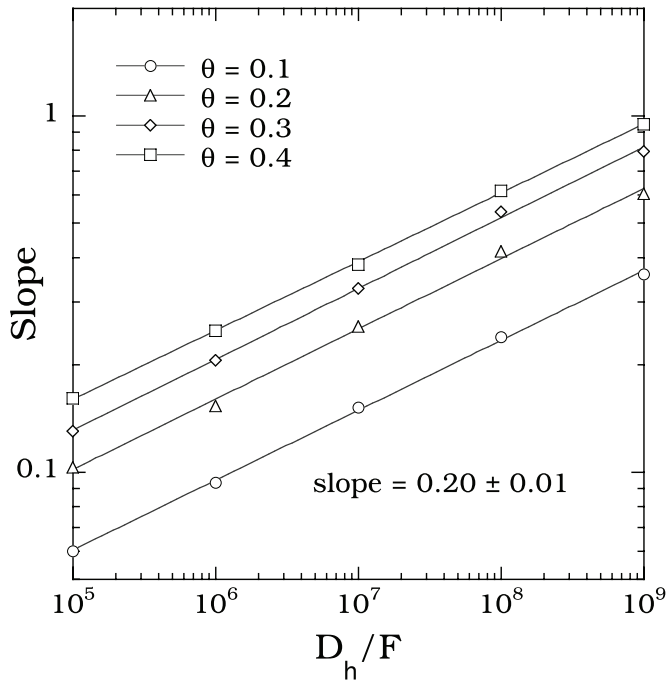


FIG. 8. Slope of scaled CZD curves at crossing point  $u_c \approx 1.5$  for  $D_h/F = 10^5 - 10^9$ , at different coverages.

ior is higher than 3, and is possibly equal to 4.

The results presented here appear to confirm this prediction since in general we have found excellent agreement between our KMC results and our self-consistent MF RE calculations in  $d=4$ . In particular, our results for the exponent describing the divergence of the peak height of the scaled ISD as a function of  $D/F$  are in excellent agreement with the MF RE results, while an analysis of the  $D/F$  dependence of the peak position indicates an asymptotic divergence at a scaled island size  $u=3/2$  in good agreement with the MF prediction. Our KMC results also indicate that at finite coverage the scaled CND approaches the MF result  $C(u)=1$  for  $0 < u < 3/2$  in the asymptotic limit of large  $D/F$ . Thus, we conclude that the critical dimension for irreversible nucleation and growth of point islands is equal to 4.

In this connection it is interesting to compare our results with previous results obtained for the case of irreversible aggregation [34–36] in which it was found that the upper critical dimension is 2. This implies that fluctuations play an important role for  $d < 2$  while there are logarithmic corrections in 2D. If one only considers average quantities such as the average island and monomer density, then in the asymptotic limit of large  $D/F$  the same is true for the irreversible nucleation and growth of point islands. In particular,

for  $d=3$  [33] and 4 the asymptotic average capture number  $\sigma_{av}$  is a dimension-dependent constant which is independent of island size  $s$ , coverage or  $D/F$ . (In contrast, for  $d=2$  the asymptotic average capture number may be written [17] as  $\sigma_{av} \sim 1/\ln[(D/F)N_1]$  where  $N_1$  decreases with increasing  $D/F$  and coverage.) However, if one considers the island-size and/or CND, then the results of Ref. [19] ( $d=2$ ) and Ref. [33] ( $d=3$ ) indicate that due to correlations, for  $d < 4$  the scaled ISD and CND *do not agree* with the MF prediction even in the asymptotic limit of large  $D/F$ . Thus, as indicated by the results presented here, the critical dimension for irreversible nucleation and growth is  $d=4$ .

We note that, recently, somewhat similar results have also been obtained in simulations of coalescence and coarsening of adlayer clusters [37]. In this particular case, it was found that in  $d=2$  there were significant deviations from MF theory for the scaled cluster-size distribution and the cluster-cluster correlation function. Thus, one may conclude that, as for irreversible nucleation and growth, for the case of irreversible aggregation via cluster diffusion and coalescence, the critical dimension may also be larger than 2. We note, however, that, due to the fact that all clusters diffuse in cluster-cluster aggregation, the correlations are significantly weaker than for the case of irreversible nucleation and growth.

Finally, we note that it would also be interesting to compare our results with those obtained for a more realistic extended island model in  $d=4$ . For such a model, the corresponding explicit size dependence of the capture number and direct impingement terms is likely to lead to modified scaling behavior for the ISD and CND. In this connection we note that the ratio of the average island radius  $R \sim S^{1/d}$  (where  $d=4$ ) to the average island distance  $l \sim N^{-1/d}$  may be written  $R/l \sim \theta^{1/d}$ . Thus, for coverages significantly larger than  $10^{-4}$  the point-island model is not a good approximation. However, in the asymptotic limit of large  $D/F$ , there will still be a significant range of coverage  $\theta_x < \theta \ll 10^{-4}$  beyond the “nucleation coverage”  $\theta_x \sim (D/F)^{-1/2}$ , such that the mean island distance is significantly larger than the mean island radius, and the point-island model is still a good approximation. Accordingly, we expect that for such a more realistic model the scaled ISD will still diverge in the asymptotic limit of large  $D/F$ .

## ACKNOWLEDGMENTS

This work was supported by the NSF through Grants No. DMR-0219328 and No. CCF-0428826. We would also like to acknowledge grants of computer time from the Ohio Supercomputer Center (Grant No. PJS0245).

- [1] J. A. Strosio and D. T. Pierce, Phys. Rev. B **49**, R8522 (1994).
- [2] J. A. Strosio, D. T. Pierce, and R. A. Dragoset, Phys. Rev. Lett. **70**, 3615 (1994).
- [3] H. Brune, H. Roder, C. Boragno, and K. Kern, Phys. Rev. Lett.

**73**, 1955 (1994).

- [4] Z. Y. Zhang and M. G. Lagally, Science **276**, 377 (1997).
- [5] J.-K. Zuo and J. F. Wendelken, Phys. Rev. Lett. **78**, 2791 (1997).
- [6] B. Muller *et al.*, Phys. Rev. Lett. **80**, 2642 (1998).

- [7] M. Zinke-Allmang, *Thin Solid Films* **346**, 1 (1999).
- [8] B. Fischer, H. Brune, J. V. Barth, A. Fricke, and K. Kern, *Phys. Rev. Lett.* **82**, 1732 (1999).
- [9] I. Furman *et al.*, *Phys. Rev. B* **62**, R10649 (2000).
- [10] R. Ruiz *et al.*, *Phys. Rev. Lett.* **91**, 136102 (2003).
- [11] J. A. Venables, *Philos. Mag.* **27**, 697 (1973).
- [12] J. A. Venables, G. D. Spiller, and M. Hanbucken, *Rep. Prog. Phys.* **47**, 399 (1984).
- [13] M. C. Bartelt and J. W. Evans, *Phys. Rev. B* **46**, 12675 (1992).
- [14] M. C. Bartelt and J. W. Evans, *J. Vac. Sci. Technol. A* **12**, 1800 (1994).
- [15] J. G. Amar, F. Family, and P. M. Lam, *Phys. Rev. B* **50**, 8781 (1994).
- [16] C. Ratsch, A. Zangwill, P. Smilauer, and D. D. Vvedensky, *Phys. Rev. Lett.* **72**, 3194 (1994).
- [17] G. S. Bales and D. C. Chrzan, *Phys. Rev. B* **50**, 6057 (1994).
- [18] J. G. Amar and F. Family, *Phys. Rev. Lett.* **74**, 2066 (1995).
- [19] M. C. Bartelt and J. W. Evans, *Phys. Rev. B* **54**, R17359 (1996).
- [20] J. A. Blackman and P. A. Mulheran, *Phys. Rev. B* **54**, 11681 (1996).
- [21] P. A. Mulheran and J. A. Blackman, *Surf. Sci.* **376**, 403 (1997).
- [22] P. A. Mulheran and D. A. Robbie, *Europhys. Lett.* **49**, 617 (2000).
- [23] J. G. Amar, M. N. Popescu, and F. Family, *Phys. Rev. Lett.* **86**, 3092 (2001).
- [24] M. N. Popescu, J. G. Amar, and F. Family, *Phys. Rev. B* **64**, 205404 (2001).
- [25] J. G. Amar, M. N. Popescu, and F. Family, *Surf. Sci.* **491**, 239 (2001).
- [26] J. W. Evans and M. C. Bartelt, *Phys. Rev. B* **63**, 235408 (2001).
- [27] J. W. Evans and M. C. Bartelt, *Phys. Rev. B* **66**, 235410 (2002).
- [28] J. A. Venables and H. Brune, *Phys. Rev. B* **66**, 195404 (2002).
- [29] J. G. Amar and M. N. Popescu, *Phys. Rev. B* **69**, 033401 (2004).
- [30] P. A. Mulheran, *Europhys. Lett.* **63**, 379 (2004).
- [31] M. von Smoluchowski, *Z. Phys.* **17**, 557 (1916); *Z. Phys. Chem.* **92**, 129 (1917).
- [32] *Kinetics of Aggregation and Gelation*, edited by F. Family and D. P. Landau (North-Holland, Amsterdam, 1984).
- [33] F. Shi, Y. Shim, and J. G. Amar, *Phys. Rev. B* **71**, 245411 (2005).
- [34] K. Kang and S. Redner, *Phys. Rev. A* **30**, 2833 (1984).
- [35] K. Kang, S. Redner, P. Meakin, and F. Leyvraz, *Phys. Rev. A* **33**, 1171 (1986).
- [36] P. G. J. van Dongen, *Phys. Rev. Lett.* **63**, 1281 (1989).
- [37] D. S. Sholl and R. T. Skodje, *Physica A* **231**, 631 (1996).